Current and Voltage Mode Multiphase Sinusoidal Oscillators Using CBTAs

Mehmet SAGBAS[1], Umut Engin AYTEN[2], Norbert HERENCSAR[3], Shahram MINAEI[4]

[1] Dept. of Electrical-Electronics Engineering, Yeni Yuzyil University, Zeytinburnu, 34010 Istanbul, Turkey
[2] Dept. of Electronics and Comm. Engineering, Yildiz Technical University, Esenler, 34222, Istanbul, Turkey
[3] Dept. of Telecommunications, Brno University of Technology, Purkynova 118, 612 00 Brno, Czech Republic
[4] Dept. of Electronics and Communications Engineering, Dogus University, Acibadem, Kadikoy 34722, Istanbul, Turkey

sagbas@gmail.com, ayten@yildiz.edu.tr, herencsn@feec.vutbr.cz, sminaei@dogus.edu.tr

Abstract. *Current-mode (CM) and voltage-mode (VM) multiphase sinusoidal oscillator (MSO) structures using current backward transconductance amplifier (CBTA) are proposed. The proposed oscillators can generate n current or voltage signals (n being even or odd) equally spaced in phase. $n+1$ CBTAs, n grounded capacitor and a grounded resistor are used for nth-state oscillator. The oscillation frequency can be independently controlled through transconductance (g_m) of the CBTAs which are adjustable via their bias currents. The effects caused by the non-ideality of the CBTA on the oscillation frequency and condition have been analyzed. The performance of the proposed circuits is demonstrated on third-stage and fifth-stage MSOs by using PSPICE simulations based on the 0.25 μm TSMC level-7 CMOS technology parameters.*

Keywords

Multiphase sinusoidal oscillator, current backward transconductance amplifier (CBTA), current-mode circuits, voltage-mode circuits, active networks.

1. Introduction

Design of multiphase sinusoidal oscillators (MSOs) has received great deal of attention in the fields of communications, signal processing, and power controllers. Numerous techniques for designing a MSO have been developed in the past two decades [1]-[17]. The circuits in [1]-[3] use operational amplifiers (op-amps) as active elements while the MSO circuits in [4]-[7] employ second-generation current conveyors (CCIIs). The main drawback of the circuits in [1]-[7] is use of excessive number of resistors/capacitors. Moreover, in circuit of [1]-[3] some of the passive elements are connected in floating form which is not desirable from integrated circuit implementation point of view. There are also MSO circuits based on using current differencing transconductance amplifiers (CDTAs) [8]-[12] which all of them operate in current-mode (CM) (i.e. the output signals are currents). While the circuit in [8] has the advantage of using only grounded capacitors, the circuits in [9]-[10] employ floating capacitors/resistors. In addition the circuit in [9] requires excessive number of active elements (two for each phase) which increases the total power consumption. The MSO circuits of [11]-[12] employ multi-output CDTAs which increases the complexity of the active elements as well as the total power consumption.

There are also MSO circuits based on current differencing buffered amplifier (CDBA) [13], and current amplifiers [14]. Moreover, CM MSOs circuits using bipolar junction transistors (BJTs) have been recently introduced in [15]-[17]. However due to the use of BJT technology the oscillation frequency is strictly temperature-dependent.

The most important features in the design of a MSO circuit can be summarized as follows:

(a) Number of active component per phase,
(b) Number of $R+C$ per phase,
(c) Use of only grounded C,
(d) Use of only grounded R,
(e) Realizing odd and even number of phase,
(f) Electronic tunability,
(g) Free of matching between passive components,
(h) Low-output impedance for VM,
(i) High-output impedance for CM.

In this paper we present novel voltage-mode (VM) and current-mode (CM) MSOs with an arbitrary n number of the signals equally spaced in phase. They are constructed by cascading lossy integrators and an inverting amplifier implemented with a recently introduced active element namely current backward transconductance amplifier (CBTA). Therefore, $n+1$ CBTAs, n grounded capacitors and one grounded resistor are used for realizing n-state oscillators. A comprehensive comparison of the proposed MSO circuit and previously reported ones based on the above mentioned features is given in Tab. 1.

Ref.	(a)	(b)	(c)	(d)	(e)	(f)	(g)	(h)	(i)
[1]	1	3+1	Yes	No	Yes	No	No	Yes	NA
[2]	1	2+1	No	No	No	No	No	Yes	NA
[3]	1	3+1	No	No	Yes	No	No	Yes	NA
[5]	1	2+1	Yes	Yes	No	No	No	No	NA
[6]	1	1+2	Yes	Yes	No	No	No	No	NA
[7]	1	2+1	Yes	No	Yes	No	No	No	NA
[8]	1	0+1	Yes	*	Yes	Yes	Yes	NA	Yes
[9]	2	0+1	No	*	Yes	Yes	Yes	NA	Yes
[10]	1	2+1	No	No	Yes	Yes	Yes	NA	Yes
[11]	1	0+1	Yes	No	Yes	Yes	Yes	NA	Yes
[12]	1	1+1	Yes	Yes	No	Yes	Yes	NA	Yes
[13]	1	2+1	Yes	No	Yes	No	No	Yes	NA
[14]	1	0+1	Yes	*	No	Yes	Yes	NA	Yes
[16]	1	0+1	Yes	*	No	Yes	Yes	NA	Yes
[17]	1	0+1	Yes	*	Yes	Yes	Yes	NA	Yes
Proposed VM MSO	1	0+1	Yes	Yes	Yes	Yes	Yes	Yes	NA
Proposed CM MSO	1	0+1	Yes	Yes	Yes	Yes	Yes	NA	Yes

Tab. 1. Comparison with previously published MSOs (*: No use of external resistor, NA: Not applicable).

2. Current Backward Transconductance Amplifier

CBTA as a new active component was introduced in 2010 to provide new possibilities in the circuit synthesis [18]. Several analog signal processing applications using this active element have been reported in the literature [18]-[27]. The circuit symbol of the CBTA is shown in Fig. 1, where p and n are input terminals, and w, z are output terminals. This active element is equivalent to the circuit in Fig. 1(b), which involves dependent current and voltage sources. The CBTA terminal equations can be defined as:

$$I_z = g_m(s)(V_p - V_n),\ V_w = \mu_w(s)V_z,\ I_p = \alpha_p(s)I_w,\ I_n = -\alpha_n(s)I_w \quad (1)$$

where $\alpha_p(s)$, $\alpha_n(s)$ and $\mu_w(s)$ are respectively the current and voltage gains ideally equal to unity. These parameters can be expressed as $\alpha_p(s) = \omega_{ap}(1 - \varepsilon_{ap})/(s + \omega_{ap})$, $\alpha_n(s) = \omega_{an}(1 - \varepsilon_{an})/(s + \omega_{an})$, $\mu_w(s) = \omega_\mu(1 - \varepsilon_\mu)/(s + \omega_\mu)$ with $|\varepsilon_{ap}| << 1$, $|\varepsilon_{an}| << 1$, and $|\varepsilon_\mu| << 1$. In addition $g_m(s) = g_o\omega_{gm}(1 - \varepsilon_{gm})/(s + \omega_{gm})$ where $|\varepsilon_{gm}| << 1$. Here, g_o is the DC transconductance gain, ε_{ap} and ε_{an} denote the current tracking errors, ε_μ denotes the voltage tracking error, ε_{gm} denotes the transconductance error and ω_{ap}, ω_{an}, ω_{gm}, ω_μ denote the corner frequencies.

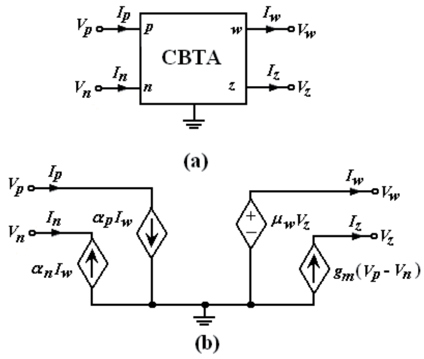

Fig. 1. (a) Block diagram of CBTA, (b) equivalent circuit of the CBTA.

The number of z-output terminals of the CBTA can be increased easily by extending current mirrors used in its internal structure. In this case, the currents of the copied z terminals (z_c) are defined as $I_{zc} = g_m(s)(V_p - V_n)$. Meanwhile, the voltage at w terminal is dependent only to the z terminal.

The CMOS implementation of the CBTA is given in Fig. 2 [23]. The dimensions of the MOS transistors used in the CBTA implementation are given in Tab. 2. As seen from Fig. 2, the transistors M_{21}–M_{34} are used for realizing the transconductance section, and the transistors M_{35}–M_{42} are used for realizing the z-copy current section, while transistors M_1–M_{14} form a current conveyor. In addition transistors M_{15}–M_{19} are employed for biasing purpose. v_{in} is the differential input voltage ($v_{in} = v_p - v_n$), i_o is the output current of the transconductance section and I_B is the bias current. The gain of the current mirrors in the output stage of the transconductance section is set to 4. Therefore, the output current i_o can be found as:

$$i_o = g_m v_{in} = \left(4 \times \sqrt{I_B \mu C_{ox} \frac{W_{21,22}}{L_{21,22}}}\right) v_{in} \quad (2)$$

where μ is the mobility of the carrier, C_{ox} is the gate-oxide capacitance per unit area, $W_{21,22}$ is the effective channel width, $L_{21,22}$ is the effective channel length of the transistors M_{21}-M_{22}.

PMOS Transistors	W(μm)/L(μm)
M_3–M_9	20/1
M_{15}	1/0.25
M_{16}, M_{17}, M_{23}–M_{27}, M_{29}	2.5/0.25
M_{28}, M_{30}, M_{35}–M_{38}	10/0.25
NMOS Transistors	W(μm)/L(μm)
M_1, M_2, M_{13}, M_{14}	10/1
M_{10}–M_{12}	2.5/1
M_{18}, M_{19}	0.5/0.25
M_{20}	2.5/0.25
M_{21}, M_{22}	2/0.25
M_{31}, M_{32}	2.25/0.25
M_{33}, M_{34}, M_{39}–M_{42}	10/0.25

Tab. 2. Dimension of the CMOS transistors.

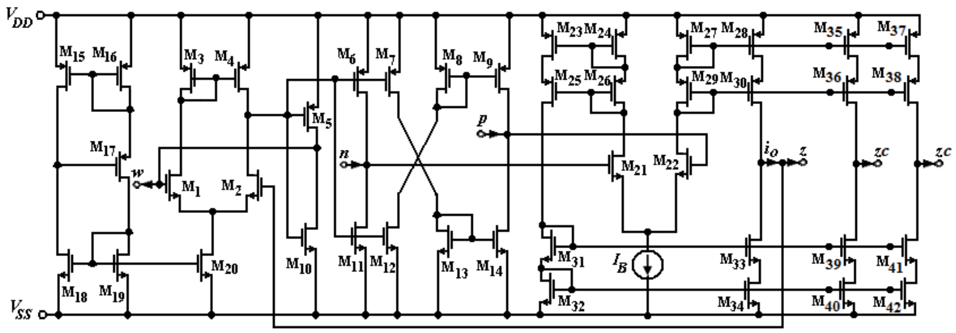

Fig. 2. CMOS implementation of CBTA.

3. CBTA-Based MSOs

The generalized structure of an n-phase sinusoidal oscillator is shown in Fig. 3 [1], [2], [4], [7]. It consists of n cascaded lossy integrators and a unity gain inverting amplifier in a closed loop. For lossy integrator sections k is the low-frequency stage gain, and T is the system time constant [1]. The system loop gain is given by:

$$L(s) = \frac{V_{on}(s)}{V_{ix}(s)} = -\left(\frac{k}{1+Ts}\right)^n . \tag{3}$$

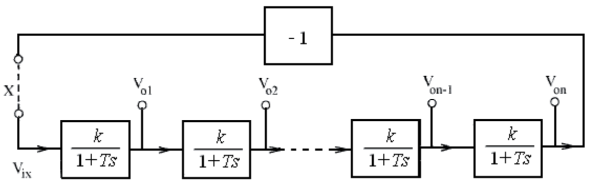

Fig. 3. Generalized block diagram of an n-phase sinusoidal oscillator.

For oscillation to sustain, the Barkhausen criteria must be satisfied [28]:

$$-\left(\frac{k}{1+Ts}\right)^n \Bigg|_{s=j\omega_o} = 1 . \tag{4}$$

That is

$$(1+j\omega_o T)^n + k^n = 0 . \tag{5}$$

Equation (5) can be rewritten as:

$$(1+\omega_o^2 T^2)^{n/2} \cdot e^{jn\cdot\tan^{-1}\omega_o T} = k^n \cdot e^{j\pi} . \tag{6}$$

Thus the oscillation condition (OC) and oscillation frequency (OF) are found as:

$$\text{OC:}\ k = (1+\omega_o^2 T^2)^{\frac{1}{2}} , \tag{7a}$$

$$\text{OF:}\ \omega_o = \frac{1}{T}\tan\left(\frac{\pi}{n}\right) . \tag{7b}$$

Substituting ω_o of (7b) in (7a) gives:

$$\text{OC:}\ k = \left[1+\tan^2\left(\frac{\pi}{n}\right)\right]^{\frac{1}{2}} \tag{8}$$

From (8) it can be seen that the oscillation condition depends on the number of the oscillation phases, n. It is obvious that the oscillation occurs when $n \geq 3$. The output number of the oscillator is n, each output voltage V_{on} is shifted in phase by $180°/n$.

The CBTA realization of the MSO constitutes of two sub-circuits, i.e. lossy integrator and inverting amplifier shown in Fig. 4. The voltage gains of the circuits in Figs. 4(a) and 4(b) can be found respectively as:

$$\frac{V_{o_i}}{V_{o_{i-1}}} = \frac{\mu_w g_{mi}/C_i}{s+\mu_w g_{mi}/C_i} = \frac{1}{1+s\dfrac{C_i}{\mu_w g_{mi}}} \tag{9a}$$

and

$$\frac{V_o}{V_i} = -\mu_w g_{mf} R_f = -K \tag{9b}$$

where g_{mf} is the transconductance of the CBTA used in the inverting amplifier of Fig. 4(b). Moreover, from (9b) $K = \mu_w g_{mf} R_f$ is the gain (in magnitude) of the VM inverting amplifier shown in Fig. 4(b).

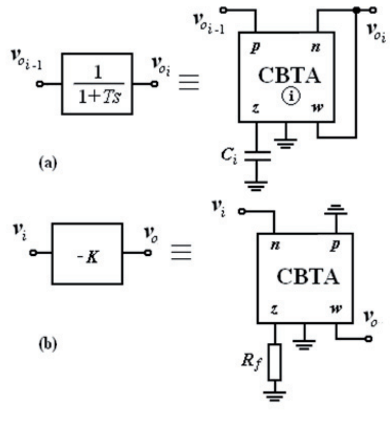

Fig. 4. Sub-circuits and their realization using CBTA: (a) VM lossy integrator, (b) VM inverting amplifier.

The general realization of arbitrary n-phase sinusoidal oscillator can be easily realized by interconnecting the above CBTA-based sub-circuits as shown in Fig. 5a. The resulting VM circuit is shown in Fig. 5b.

The closed loop gain of the circuit in Fig. 5(b) can be expressed as:

$$L(s) = -\mu_w g_{mf} R_f \left[\frac{1}{1 + s\dfrac{C_i}{\mu_w g_{mi}}} \right]^n = -K \left[\frac{1}{1 + s\dfrac{C_i}{\mu_w g_{mi}}} \right]^n . \quad (10)$$

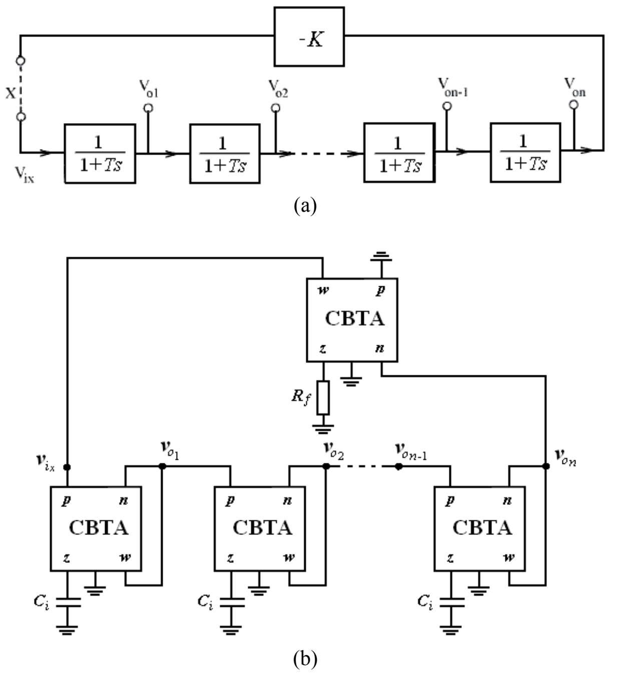

Fig. 5. (a) Generalized block diagram of the proposed n-phase sinusoidal oscillator. (b) Proposed voltage-mode CBTA-based MSO.

For oscillation to sustain, the Barkhausen criteria must be satisfied, that is:

$$-K \left[\frac{1}{1 + s\dfrac{C_i}{\mu_w g_{mi}}} \right]^n = 1 . \quad (11)$$

Therefore, the oscillation condition and the oscillation frequency are found from (11) as:

$$\text{OC: } K = \left(1 + \frac{\omega_o^2 C_i^2}{\mu_w^2 g_{mi}^2} \right)^{n/2} , \quad (12a)$$

$$\text{OF: } \omega_o = \frac{\mu_w g_{mi}}{C_i} \tan\left(\frac{\pi}{n} \right). \quad (12b)$$

Substituting ω_o of (12b) into (12a) gives:

$$\text{OC: } K = \left[1 + \tan^2 \left(\frac{\pi}{n}\right) \right]^{n/2} \quad (13)$$

Further, from (12b) and (13) it can be seen that the oscillation frequency can be independently controlled through equal valued g_{mi} parameters which are electronically adjustable by changing the bias currents of the CBTAs.

The output impedance of the proposed structure can be found as:

$$Z_{o_i} = Z_{n_i} // Z_{p_{i+1}} // Z_{w_i} . \quad (14)$$

In ideal case $Z_{w_i} = 0$, thus $Z_{o_i} = 0$.

The second proposed CBTA-based MSO circuit which operates in current-mode can be obtained using two sub-circuits shown in Fig. 6.

The current gains of the circuits in Figs. 6(a) and 6(b) can be found respectively as follows:

$$\frac{I_{o_i}}{I_{o_{i-1}}} = \frac{\alpha_n g_{mi} / C_i}{s + g_{mi} / C_i} = \frac{\alpha_n}{1 + sC_i / g_{mi}} \quad (15a)$$

and

$$\frac{I_o}{I_i} = -g_{mf} R_f = -K \quad (15b)$$

where g_{mf} is the transconductance of the CBTA used in the inverting amplifier of Fig. 6(b). From (15b) $K = g_{mf} R_f$ which is the gain of the CM inverting amplifier shown in Fig. 6(b).

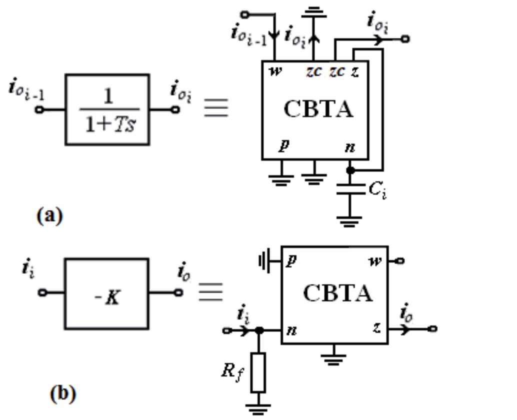

Fig. 6. Sub-circuits and their realization using CBTA: (a) CM lossy integrator, (b) CM inverting amplifier.

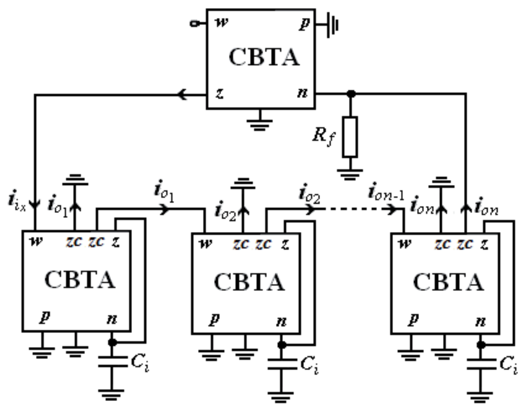

Fig. 7. Proposed current-mode CBTA-based MSO.

The general realization of arbitrary n-phase sinusoidal oscillator can be easily realized by interconnecting the above CBTA-based sub-circuits in accordance to the block diagram of Fig. 3. The resulting circuits are shown in Fig. 7. The closed loop gains of the circuits in Fig. 7 can be expressed as:

$$L(s) = -g_{mf} R_f \left[\frac{\alpha_n}{1 + sC_i / g_{mi}} \right]^n = -K \left[\frac{\alpha_n}{1 + sC_i / g_{mi}} \right]^n . \quad (16)$$

For oscillation to sustain, the Barkhausen criteria must be satisfied, that is:

$$-K \left[\frac{\alpha_n}{1 + sC_i / g_{mi}} \right]^n = 1 \quad (17)$$

Therefore, the oscillation condition and the oscillation frequency are found from (17) as:

$$\text{OC: } K = \alpha_n^{-n} \left(1 + \frac{\omega_o^2 C_i^2}{g_{mi}^2} \right)^{\frac{n}{2}}, \quad (18a)$$

$$\text{OF: } \omega_o = \frac{g_{mi}}{C_i} \tan\left(\frac{\pi}{n}\right). \quad (18b)$$

Substituting ω_o of (18b) into (18a) gives OC:

$$K = \alpha_n^{-n} \left[1 + \tan^2\left(\frac{\pi}{n}\right) \right]^{\frac{n}{2}}. \quad (19)$$

Again from (18b) and (19) it can be realized that the oscillation frequency can be independently controlled through equal valued g_{mi} parameters which are electronically adjustable by changing the bias currents of the CBTAs.

The output impedance of the proposed structure can be found as:

$$Z_{oi} = R_{zi} // (1/sC_{zi}), \quad i = 1,2,\ldots,n \quad (20)$$

where R_z and C_z are the z-terminal resistances and capacitance of the CBTAs. In ideal case $Z_{oi} = \infty$.

4. Simulation Results

To verify the proposed MSOs, the CBTAs are simulated using the CMOS-based CBTA circuit shown in Fig. 2 with DC power supply voltages equal to $V_{DD} = -V_{SS} =$ 1.5 V. The simulations are performed by using the PSPICE based on 0.25 μm level-7 TSMC CMOS technology parameters. Some of the technology parameters used in PSPICE simulations are given as follows: threshold voltage $V_{TH0} = 0.3894$ V, low field mobility $U_0 = 302.356$ cm^2/Vs, and gate oxide thickness $T_{ox} = 5.714 \cdot 10^{-9}$ m for the NMOS transistor in addition to $V_{TH0} = -0.567$ V, $U_0 =$ 107.1614 cm^2/Vs, and $T_{ox} = 5.714 \cdot 10^{-9}$ m for the PMOS transistor.

In this simulation, the voltage-mode MSO circuit of Fig. 5(b) for $n = 3$ is designed with the passive component values of $C_1 = C_2 = C_3 = 50$ pF and $R_f = 16$ kΩ, all bias currents of the CBTAs are chosen as 50 μA ($g_m = 0.5$ mS).

Fig. 8 shows the voltage outputs of each stage in the MSO. In this case ($n = 3$) with all the above parameters, the oscillation frequency is obtained as 2.56 MHz from the simulation which is close to the theoretical value of 2.756 MHz. The phase differences among the outputs for $n = 3$ is in the vicinity of 120 degree. It should be mentioned that no amplitude limiter circuit is used so the output voltage at v_{o1} is a little distorted. The THD values for v_{o1}, v_{o2}, v_{o3} voltage outputs are 2.1%, 1.7% and 0.75%, respectively.

The simulation results for $n = 5$ with same component values (except R_f which is 5.8 kΩ) is also given in Fig. 9. The oscillation frequency is obtained as 1.13 MHz from the simulation which is close to the theoretical value of 1.156 MHz.

The FFT spectrum of the each output signals for $n = 3$ are shown in Figs. 10-12. As seen from Figs. 8-12, the oscillations are observed to be quite stable and the simulation results confirm the workability of the proposed oscillator circuit.

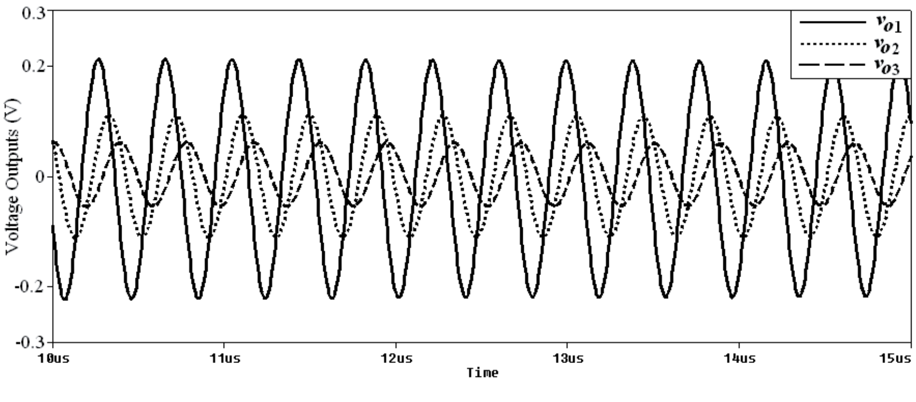

Fig. 8. Output voltages of the proposed VM MSO for $n = 3$.

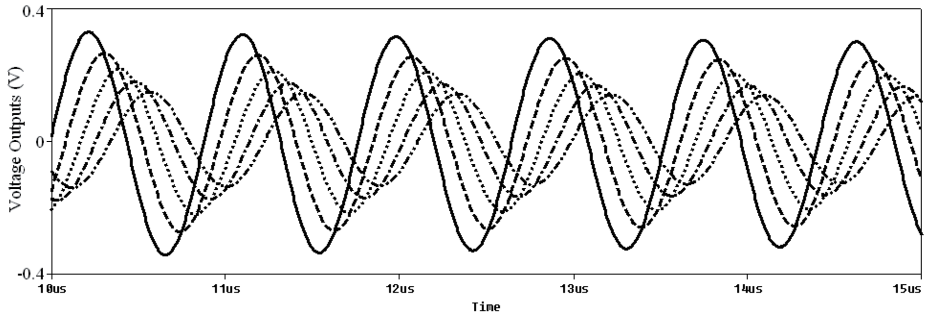

Fig. 9. Output voltages of the proposed VM MSO for $n = 5$.

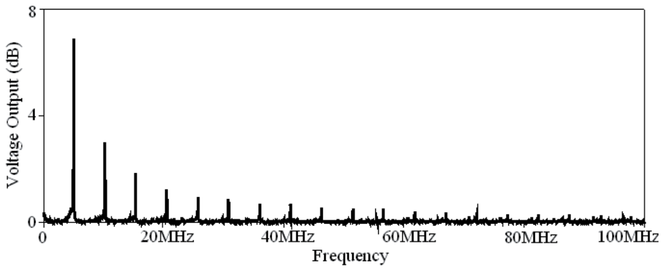

Fig. 10. FFT spectrum of the sinusoidal voltage output v_{o1}.

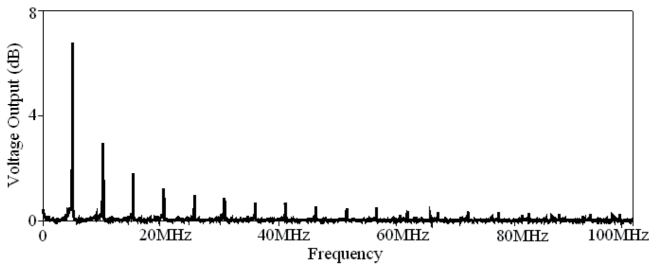

Fig. 11. FFT spectrum of the sinusoidal voltage output v_{o2}.

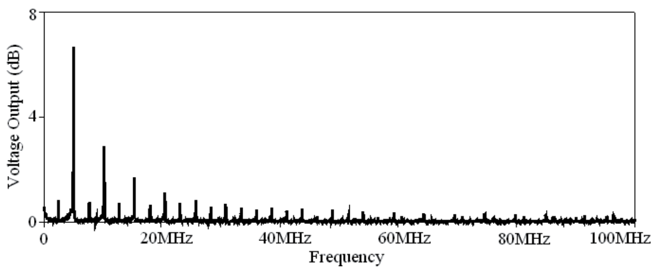

Fig. 12. FFT spectrum of the sinusoidal voltage output v_{o3}.

For the current-mode MSO circuit, the simulations are repeated. The MSO circuit for $n = 3$ is designed with the passive component values $C_1 = C_2 = C_3 = 10$ pF and $R_f = 16$ kΩ, all bias currents of the CBTAs are chosen as 50 μA ($g_m = 0.5$ mS).

Fig. 13 shows the current outputs of each stage in the MSO. In this case ($n = 3$) with all the above parameters, the oscillation frequency is obtained as 10.8 MHz from the simulation while the theoretical value is 13.77 MHz. The difference between theoretical and simulated values can be attributed to the parasitic effects of the CBTAs. The phase differences among the outputs for $n = 3$ is in the vicinity of 120 degree. The THD values for i_{o1}, i_{o2}, i_{o3} voltage outputs are 5.57%, 1.93% and 0.98%, respectively. The FFT spectrum of the each current output signals for $n = 3$ are shown in Fig. 14. As seen from Figs. 13 and 14, the oscillations are observed to be quite stable and the simulation results confirm the workability of the proposed current-mode oscillator circuit.

Due to the non-idealities of the CBTA, some discrepancies exhibit between theoretical and simulation results as shown in Figs. 8-14. In order to find operating point and non-idealities of CBTA, the PSPICE simulations are also done by using above mentioned transistor model. As a result, corner frequencies are $\omega_{ap} = 5300$, $\omega_{an} = 6000$, $\omega_{gm} = 5000$ and $\omega_{\mu} = 3015$ Mrad/s and errors of these gains are $\varepsilon_{ap} = -0.0142$, $\varepsilon_{an} = 0.003$, $\varepsilon_{gm} = 0.0184$ and $\varepsilon_{\mu} = -0.0035$. For low-frequency application α_p, α_n, g_m and μ_w can be assumed to be the constants with values $1-\varepsilon_{ap} = 1.0142$, $1-\varepsilon_{an} = 0.997$, $1-\varepsilon_{gm} = 1.9816$ and $1-\varepsilon_{\mu} = 1.0035$, respectively.

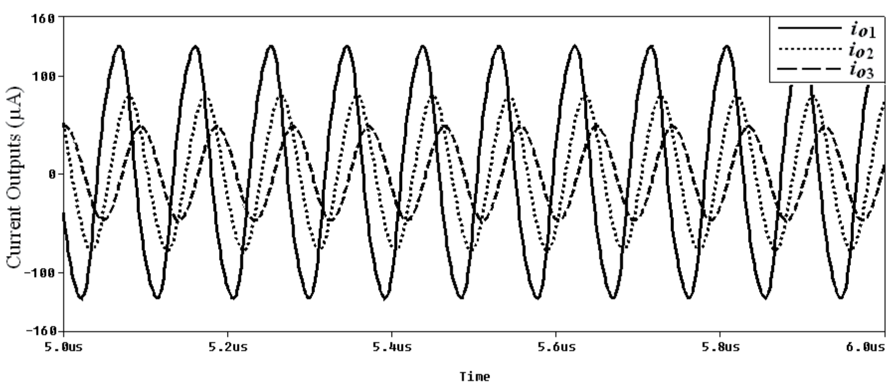

Fig. 13. Current outputs of the proposed CM MSO for $n = 3$.

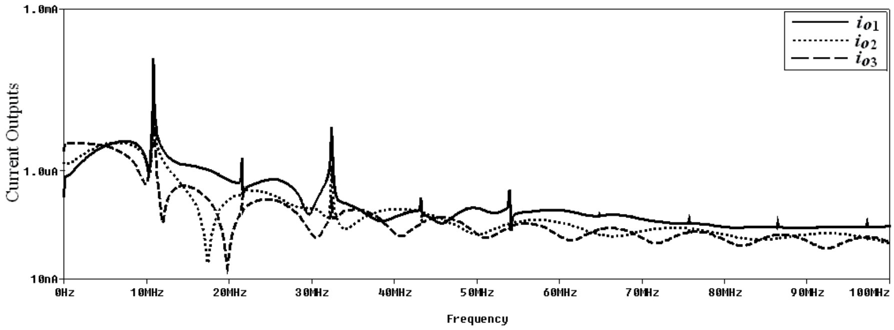

Fig. 14. FFT spectrum of the sinusoidal current outputs.

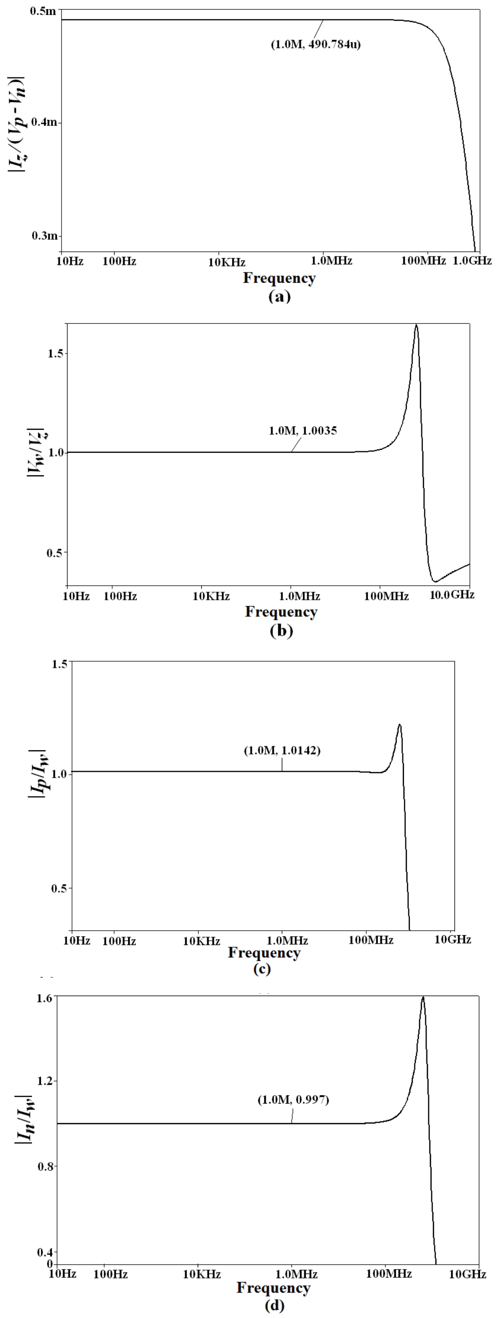

Fig. 15. Variation of a) the transconductance gain, b) voltage gain c), d) currents gain of the CBTA versus frequency.

Therefore, the maximum operating frequency of the CBTA can be found as follows $f_{\max} = \min\{f_{\alpha p}, f_{\alpha n}, f_{gm}, f_{\mu}\} \approx 480$ MHz. The frequency responses of the transconductance gain $|g_m| = |I_z/(V_p - V_n)|$, the voltage gain $|\mu_w| = |V_w/V_z|$, and the current gains $|\alpha_p| = |I_p/I_w|$, $|\alpha_n| = |I_n/I_w|$ are given in Figs. 15 (a-d), respectively.

The DC transconductance transfer characteristic of i_z against v_p-v_n when $g_m = 0.5$ mS, and DC voltage transfer characteristic of v_w against v_z are shown in Fig. 16a. For this simulation, a DC voltage sweep between $-1\text{ V} \le (v_p - v_n) \le 1$ V was applied to the p and n terminals of the CBTA. The output z terminal current is measured while 1 TΩ resistor is connected to the w output of the CBTA and the output z terminal is grounded. As a result, the CBTA works linearly between $-200\ \mu\text{A} \le i_z \le 200\ \mu$A and $-0.4\text{ V} \le v_p - v_n \le 0.4$ V with an error less than 1 % for $g_m = 0.5$ mS.

The DC characteristics such as plots of v_w against v_z for the proposed CBTA are obtained as shown in Fig. 16b. For this simulation, a DC voltage sweep between $-2\text{ V} \le v_z \le 1.5$ V is applied to the z terminal of the CBTA. The output w terminal voltage is measured while 1 TΩ resistor is connected to the w output of the CBTA and the p and n terminals are grounded. As a result, the CBTA works linearly between $-1.5\text{ V} \le v_w \le 1$ V with an error less than 1 % for $g_m = 0.5$ mS.

The DC current transfer characteristics of i_p and i_n against i_w for the proposed CBTA are obtained as shown in Figs. 16c and 16d. For these simulations, a DC current sweep between $-1\text{ mA} \le i_w \le 1.5$ mA is applied to the w terminal of the CBTA. The input p and n terminal currents are measured while the z, p and n terminals are grounded. As a result, the CBTA works linearly between $-750\text{ mA} \le i_p \le 1.3$ mA and $-750\text{ mA} \le i_n \le 1.1$ mA with an error less than 1 % for $g_m = 0.5$ mS.

The simulation results also show that the values of the transconductance gain g_m of the CBTA are between 28 µS and 1.2 mS.

The CBTA has parasitic resistances and capacitances as shown in Fig. 17. The parasitic resistances and capacitances values of the CBTA are given in Tab. 3.

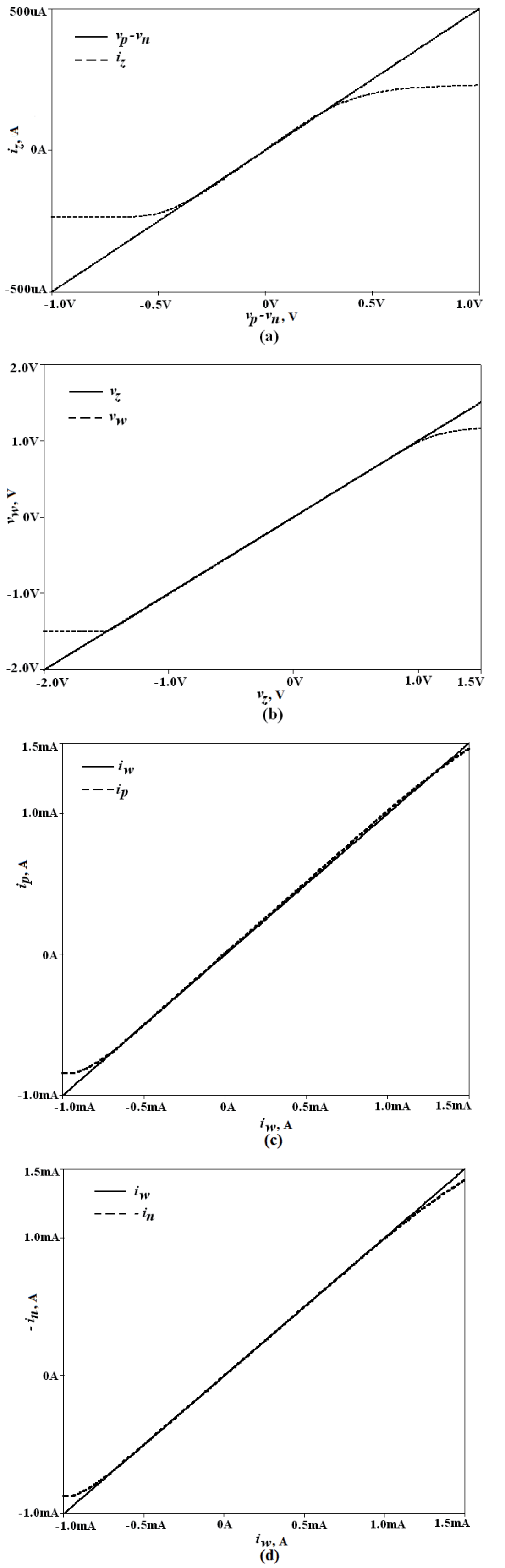

Fig. 16. a) The transconductance transfer characteristic $i_z = g_m(v_p - v_n)$, b) The voltage transfer characteristic $v_w = v_z$, c) The current transfer characteristic $i_p = i_w$, d) The current transfer characteristic $i_n = -i_w$.

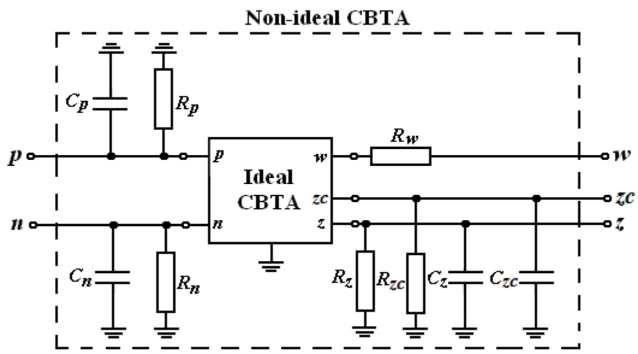

Fig. 17. Parasitic resistance and capacitance of the CBTA.

Parasitic Impedances	Values
R_p	53 kΩ
R_n	67 kΩ
R_z	403 kΩ
R_{zc}	415 kΩ
R_w	19.6 Ω
C_p	75 fF
C_n	990 fF
C_z	430 fF
C_{zc}	56 fF

Tab. 3. Parasitic impedances of the CBTA.

5. Conclusion

Novel current and voltage-mode versatile generalized n-phase sinusoidal oscillator structures using CBTAs are proposed. The proposed circuits use grounded resistors and capacitors which are suitable for IC implementations. They generate n current or voltage signals which are equally spaced in phase, n can be chosen as even or odd number. The oscillation frequency can be electronically controlled using bias currents of CBTAs.

The above properties make the proposed MSOs attractive for circuit designers and engineers.

Acknowledgements

Ing. Norbert Herencsar, Ph.D. was supported by the project CZ.1.07/2.3.00/30.0039 of Brno University of Technology. The research described in this paper was also in part supported by the project SIX CZ.1.05/2.1.00/03.0072 from the operational program Research and Development for Innovation, BUT Fund No. FEKT-S-11-15, and Czech Science Foundation projects under No. P102/11/P489, P102/10/P561, P102/09/1681. Authors also wish to thank Dr. Roman Sotner from the Brno University of Technology, Czech Republic, for his discussions made on proposed circuits.

A preliminary version of this paper has been presented at the 2012 35th International Conference on Telecommunications and Signal Processing (TSP) [29].

References

[1] GIFT, J. S. G. Multiphase sinusoidal oscillator system using operational amplifiers. *International Journal of Electronics*, 1997, vol. 83, no. 1, p. 61 - 67.

[2] GIFT, J. S. G. Multiphase sinusoidal oscillator using inverting-mode operational amplifiers. *IEEE Transactions on Instrumentation and Measurement*, 1998, vol. 47, no. 4, p. 986 to 991.

[3] MAUNDY, B., ELWAKIL, A., GIFT, S. On the realization of multiphase oscillators using fractional-order allpass filters. *Circuits, Systems, and Signal Processing*, 2012, vol. 31, no. 1, p. 3 - 17.

[4] HOU, C. L., SHEN, B. Second-generation current conveyor-based multiphase sinusoidal oscillators. *International Journal of Electronics*, 1995, vol. 78, no. 2, p. 317 - 325.

[5] WU, D.-S., LIU, S.-I., HWANG, Y.-S., WU, Y.-P. Multiphase sinusoidal oscillator using second-generation current conveyors. *International Journal of Electronics*, 1995, vol. 78, no. 4, p. 645 to 651.

[6] ABUELMA'ATTI, M. T., AL-QAHTANI, M. A. Low component second generation current conveyor-based multiphase sinusoidal oscillator. *International Journal of Electronics*, 1998, vol. 84, no. 1, p. 45 - 52.

[7] SKOTIS, G. D., PSYCHALINOS, C. Multiphase sinusoidal oscillators using second generation current conveyors. *AEU - International Journal of Electronics and Communications*, 2010, vol. 64, no. 12, p. 1178 - 1181.

[8] TANGSRIRAT, W., TANJAROEN, W. Current-mode multiphase sinusoidal oscillator using current differencing transconductance amplifiers. *Circuits, Systems, and Signal Processing*, 2008, vol. 27, no. 1, p. 81 - 93.

[9] TANGSRIRAT, W., TANJAROEN, W., PUKKALANUN, T. Current-mode multiphase sinusoidal oscillator using CDTA-based allpass sections. *AEU - International Journal of Electronics and Communications*, 2009, vol. 63, no. 7, p. 616 - 622.

[10] JAIKLA, W., SIRIPRUCHYANUN, M., BIOLEK, D., BIOLKOVA, V. High-output-impedance current-mode multiphase sinusoidal oscillator employing current differencing transconductance amplifier-based allpass filters. *International Journal of Electronics*, 2010, vol. 97, no. 7, p. 811 - 826.

[11] LI, Y. A novel current-mode multiphase sinusoidal oscillator using MO-CDTAs. *International Journal of Electronics*, 2012, vol. 99, no. 4, p. 477 - 489.

[12] JAIKLA, W., PROMMEE, P. Electronically tunable current-mode multiphase sinusoidal oscillator employing CCCDTA-based allpass filters with only grounded passive elements. *Radioengineering*, 2011, vol. 20, no. 3, p. 594 - 599.

[13] PISITCHALERMPONG, S., TANGSRIRAT, W., SURAKAM-PONTORN, W. CDBA-based multiphase sinusoidal oscillator using grounded capacitors. In *Proceeding of the SICE-ICASE International Joint Conference.* Bexco, Busan (Korea), 2006, p. 5762 - 5765.

[14] SOULIOTIS, G., PSYCHALINOS, C. Electronically controlled multiphase sinusoidal oscillators using current amplifiers. *International Journal of Circuit Theory and Applications*, 2009, vol. 37, no. 1, p. 43 - 52.

[15] PROMMEE, P., SRA-IUM, N., DEJHAN, K. High-frequency log-domain current-mode multiphase sinusoidal oscillator. *IET Circuits Devices & Systems*, 2010, vol. 4, no. 5, p. 440 - 448.

[16] UTTAPHUT, P. New current-mode multiphase sinusoidal oscillators based on CCCCTA-based lossy integrators. *Przeglad Elektrotechniczny*, 2012, vol. 88, no. 1A, p. 291 - 295.

[17] KUMNGERN, M., CHANWUTITUM, J., DEJHAN, K. Electronically tunable multiphase sinusoidal oscillator using translinear current conveyors. *Analog Integrated Circuits and Signal Processing*, 2010, vol. 65, no. 2, p. 327 - 334.

[18] AYTEN, U. E., SAGBAS, M., SEDEF, H. Current-mode leapfrog ladder filter using a new active block. *AEU - International Journal of Electronics and Communications*, 2010, vol. 64, no. 6, p. 503 to 511.

[19] SAGBAS, M., AYTEN, U. E., SEDEF, H. Current and voltage transfer function filters using a single active device. *IET Circuits Devices & Systems*, 2010, vol. 4, no. 1, p. 78 - 86.

[20] KOKSAL, M., AYTEN, U. E., SAGBAS, M. Realization of new mutually coupled circuit using CC-CBTAs. *Circuits, Systems, and Signal Processing*, 2012, vol. 31, no. 2, p. 435 - 446.

[21] KOKSAL, M. Realization of a general all-pole current transfer function by using CBTA. *International Journal of Circuit Theory and Applications*, Published online on 10 Oct. 2011. DOI: 10.1002/cta.806

[22] AYTEN, U. E., SAGBAS, M., HERENCSAR, N., KOTON, J. Novel floating FDNR, inductor and capacitor simulator using CBTA. In *Proceeding of 2011 34th International Conference on Telecommunications and Signal Processing (TSP 2011).* Budapest (Hungary), 2011, p. 312 - 316.

[23] SAGBAS, M. Component reduced floating ±L, ±C and ±R simulators with grounded passive components. *AEU - International Journal of Electronics and Communications*, 2011, vol. 65, no. 10, p. 794 - 798.

[24] HERENCSAR, N., LAHIRI, A., KOTON, J., SAGBAS, M., AYTEN, U. E., VRBA, K. New MOS-C realization of transadmittance type all-pass filter using modified CBTA. In *Proceeding of International Conference on Applied Electronics (AE 2011).* Pilsen (Czech Republic), 2011, p. 153 - 156.

[25] HERENCSAR, N., KOTON, J., VRBA, K., LAHIRI, A., AYTEN, U. E., SAGBAS, M. A new compact CMOS realization of sinusoidal oscillator using a single modified CBTA. In *Proceeding of 21st International Conference Radioelektronika.* Brno (Czech Republic), 2011, p. 41 - 44.

[26] AYTEN, U. E., SAGBAS, M., SEDEF, H. Electronically tunable sinusoidal oscillator circuit with current and voltage outputs. *International Journal of Electronics*, 2012, vol. 99, no. 8, p. 1133 to 1144.

[27] AYTEN, U. E., SAGBAS, M., HERENCSAR, N., KOTON, J. Novel floating general element simulators using CBTA. *Radioengineering*, 2012, vol. 21, no. 1, p. 11 - 19.

[28] MILLMAN, J., HALKIAS, C. C. *Integrated Electronics*. New York: McGraw-Hill, 1972.

[29] SAGBAS, M., AYTEN, U. E., HERENCSAR, N., MINAEI, S. Voltage-mode multiphase sinusoidal oscillators using CBTAs. In *Proceedings of the 2012 35th International Conference on Telecommunications and Signal Processing (TSP 2012).* Prague (Czech Republic), 2012, p. 421 - 425.

About Authors ...

Mehmet SAGBAS received his B.S. degree in Electronics Engineering from the Istanbul Technical University in 2000. He received his M.S. degree in Electronics Engi neering from the Fatih University in 2004. He received his Ph.D. degree in Electronics Engineering from the Yildiz Technical University in 2007. He is currently an Assoc. Professor at Maltepe University. His research interests are analog integrated circuits and analog signal processing.

Umut Engin AYTEN received the M.Sc. and Ph.D. degrees in Electronics Engineering from the Yildiz Technical University, Istanbul, Turkey, in 2003 and 2009, respectively. He is currently an Asst. Professor at Yildiz Technical University. His current field of research concerns analog integrated circuits, active filters, current-mode circuits and analog signal processing.

Norbert HERENCSAR received the M.Sc. and Ph.D. degrees in Electronics & Communication and Teleinformatics from Brno University of Technology (BUT), Brno, Czech Republic, in 2006 and 2010, respectively. Currently, he is an Assistant Professor at the Dept. of Telecommunications, BUT. From September 2009 through February 2010 he was an Erasmus Exchange Student with the Dept. of Electrical and Electronic Engineering, Bogazici University, Istanbul, Turkey. His research interests include analog filters, current-mode circuits, tunable frequency filter design methods, and oscillators. He is an author or co-author of about 75 research articles published in international journals or conference proceedings. Dr. Herencsar is Senior Member of the IACSIT and Member of the IAENG and ACEEE.

Shahram MINAEI received the B.Sc. degree in Electrical and Electronics Engineering from Iran University of Science and Technology, Tehran, Iran, in 1993 and the M.Sc. and Ph.D. degrees in Electronics and Communication Engineering from Istanbul Technical University, Istanbul, Turkey, in 1997 and 2001, respectively. He is currently a Professor in the Department of Electronics and Communication Engineering, Dogus University, Istanbul, Turkey. He has more than 100 publications in scientific journals or conference proceedings. His current field of research concerns current-mode circuits and analog signal processing. Dr. Minaei is a senior member of the IEEE, an associate editor of the Journal of Circuits, Systems and Computers (JCSC), and an area editor of the International Journal of Electronics and Communications (AEÜ).